Benzene-Templated Model Systems for Photosynthetic Antenna−Reaction Center Function†

Paul A. Liddell, Gerdenis Kodis, Linda de la Garza, Ana L. Moore,* Thomas A. Moore,* and Devens Gust*

Department of Chemistry and Biochemistry, Center for the Study of Early Events in Photosynthesis, Arizona State University, Tempe, Arizona 85287-1604

Received: January 22, 2004; In Final Form: April 5, 2004

A synthetic strategy for preparing artificial photosynthetic antenna−reaction center complexes based on formation of a benzene core via a Diels−Alder reaction has been applied to the preparation of a zinc porphyrin (P_{Zn})−free base porphyrin (P_{2H})−fullerene (C_{60}) molecular triad. Spectroscopic studies in 2-methyltetrahydrofuran show that excitation of the zinc porphyrin antenna moiety to form $^1P_{Zn}-P_{2H}-C_{60}$ is followed by singlet−singlet energy transfer to the free base porphyrin excitation energy trap ($\tau = 59$ ps), yielding $P_{Zn}-{}^1P_{2H}-C_{60}$. The free base porphyrin first excited singlet state decays by photoinduced electron transfer to the fullerene ($\tau = 25$ ps), producing a $P_{Zn}-P_{2H}^{\bullet+}-C_{60}^{\bullet-}$ charge-separated state. Charge shift ($\tau = 167$ ps) yields $P_{Zn}^{\bullet+}-P_{2H}-C_{60}^{\bullet-}$. This final charge-separated state is formed with quantum yields >90% following excitation of any of the three chromophores. Charge recombination in 2-methyltetrahydrofuran ($\tau = 50$ ns) occurs by an apparently endergonic process to give triplet states of the chromophores, rather than the ground state. In benzonitrile, charge recombination yields the ground state ($\tau = 220$ ns). The high efficiencies of the various energy and electron-transfer processes suggest that this molecular architecture will be useful for the design of more complex antenna−reaction center complexes.

Introduction

Although the conversion of excitation energy into useable chemical potential energy in the form of long-lived charge separation occurs in the photosynthetic reaction center, most of the sunlight used in photosynthesis is absorbed not by the reaction centers themselves but rather by antenna systems. Although all reaction center structures elucidated to date have related structural motifs, a large variety of antennas have evolved, as the habitats of different organisms can differ widely in the availability and spectral distribution of solar radiation. X-ray diffraction studies have revealed that the LH2 peripheral antennas of photosynthetic bacteria have the bacteriochlorophyll and carotenoid light-harvesting pigments arranged in a symmetric, circular motif.[1,2] This finding has spurred interest in the development of model antenna systems consisting of rings of porphyrin or related chromophores.[3] Some of these have used benzene as a template for organizing porphyrins in a hexameric array. One approach uses a relatively flexible ether linkage to join the porphyrins to the central benzene core.[4] A second has led to hexad **1** (Chart 1), which features more rigid linkages.[5,6]

In general, the structural factors controlling the rates of singlet energy transfer and photoinduced electron transfer are now understood to a degree that permits the design of photosynthetic model systems that combine antenna and reaction center function in the same molecule. For example, we have recently described two molecules in which an antenna consisting of four zinc porphyrins absorbs light and channels it to a free base porphyrin, which uses the resulting excitation energy to carry out photoinduced electron transfer to a covalently linked fullerene.[7,8] Combining an antenna structure such as **1** with a unit that could perform photoinduced electron transfer would be an interesting possibility, but the method used to synthesize **1**, metal-catalyzed trimerization of a symmetric diphenylethynyl-bridged diporphyrin, is only practical for the preparation of symmetric hexamers in which all porphyrins share the same central metal and substituents. This makes it impractical for linking arrays such as **1** to a single electron donor−acceptor unit, varying the metalation state of the porphyrins individually to allow vectorial energy transfer, varying the structures of the six chromophores to access different spectral profiles, etc.

CHART 1

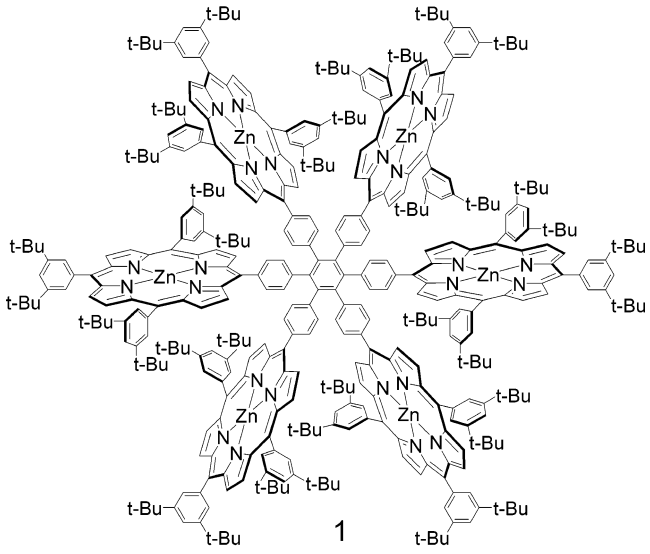

It is well-known that the reaction of diphenylacetylene and tetraphenylcyclopentadienone yields a Diels−Alder cycloaddition product that readily loses carbon monoxide to generate hexaphenylbenzene. Some time ago, we demonstrated that this

† Part of the special issue "Gerald Small Festschrift".

* Corresponding authors. E-mail: (D.G.) gust@asu.edu.

10.1021/jp040053t CCC: $27.50
Published on Web 05/28/2004

CHART 2

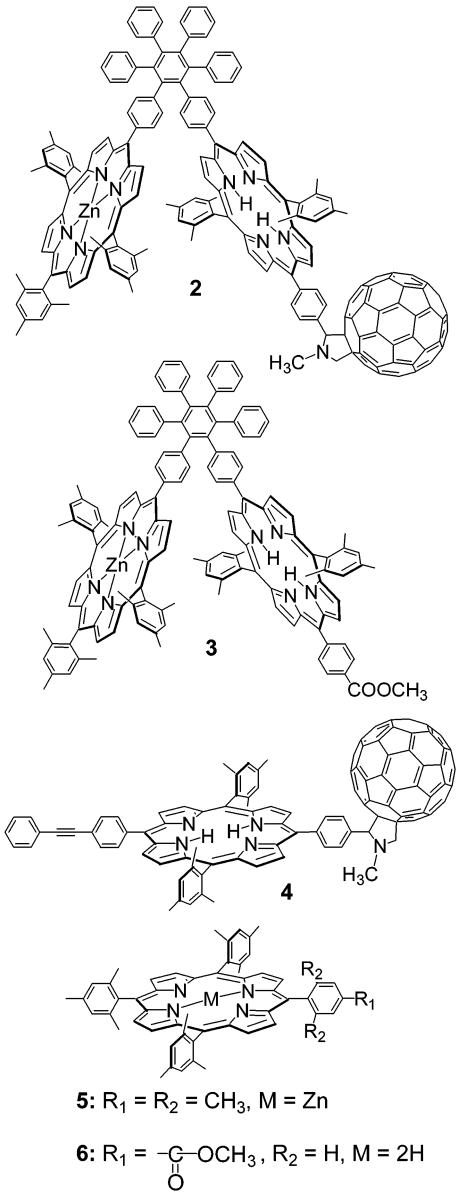

approach could be used to prepare substituted hexaarylbenzenes in which the different substituents were both sterically bulky and distributed on the hexaphenylbenzene framework in a planned, rational way.[9−11] This is possible because both the tetraarylcyclopentadienone and diarylacetylene precursors may be readily prepared in nonsymmetric forms. If the same reactions occur when the precursors bear porphyrin moieties, these methods should be applicable to the preparation of unsymmetrical multiporphyrin arrays related to **1**. As a first step in the investigation of this possibility, we now report the synthesis of zinc porphyrin (P_{Zn})−free base porphyrin (P_{2H})−fullerene (C_{60}) triad **2** and related model compounds (Chart 2) and describe their singlet energy and photoinduced electron-transfer properties.

Results

Synthesis. Dyad **3** was prepared by the Diels−Alder cycloaddition of the appropriate unsymmetrical porphyrin-bearing diarylacetylene with tetraphenylcyclopentadienone. The diarylacetylene precursor was synthesized by first coupling 5-(4-carboxymethylphenyl)-15-(4-iodophenyl)-10,20-bis(2,4,6-trimethylphenyl)porphyrin and triisopropylsilylacetylene using triphenylarsine and palladium catalysts to yield a protected alkyne bearing a single porphyrin. Next, the triisopropylsilyl protecting group was removed with tetra-*n*-butylammonium fluoride, and the coupling reaction was repeated with the resulting alkyne and 5-(4-iodophenyl)-10,15,20-tris(2,4,6−trimethyphenyl)porphyrin. The ester group of **3** was reduced to the alcohol with lithium aluminum hydride, and the alcohol was oxidized to the corresponding aldehyde with manganese dioxide. The Prato reaction[12] of the aldehyde, C_{60}, and sarcosine yielded triad **2**. The preparation of **2**, **3**, and related compounds and their characterization by NMR, mass spectrometry, and UV−vis spectrophotometry are described in detail in the Experimental Section.

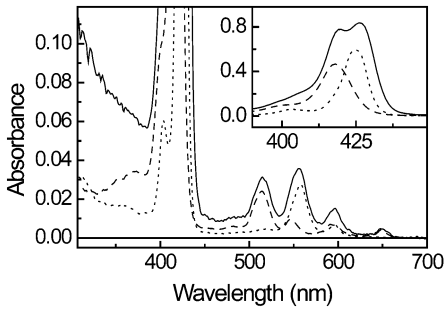

Figure 1. Absorption spectra in 2-methyltetrahydrofuran of triad **2** (−), model zinc porphyrin **5** (-----), and model free base porphyrin **6** (− − −). The inset shows the Soret region of a more dilute sample.

Cyclic Voltammetry. Cyclic voltammetric measurements were made in order to obtain redox potentials that could be used to estimate the energies of the various charge-separated states of **2** that might result from photoinduced electron-transfer reactions. The measurements were made in benzonitrile (HPLC grade) solution containing 0.1 M tetra-*n*-butylammonium hexafluorophosphate and also ferrocene as an internal redox reference material. The counter electrode was platinum, the reference electrode was Ag/0.1 M $AgNO_3$, and the working electrode was glassy carbon. Potentials are reported vs SCE.

Triad **2** exhibited reversible first and second oxidation potentials of 0.75 and 1.06 V and a reversible first reduction potential of −0.59 V. The first oxidation potential is ascribed to oxidation of the zinc porphyrin moiety and is similar to those found for structurally similar zinc porphyrins. The second oxidation potential is ascribed to the free base porphyrin and the first reduction potential to the fullerene moiety. These two values are very close to those determined for the porphyrin and fullerene moieties of dyad **4** (1.05 and −0.62 V, respectively)[7] and for related model porphyrins and fullerenes. Thus, the covalent linkages and the relatively close spatial proximity of the three chromophores do not lead to significant perturbations in their redox behavior. Using these values, the energies of the $P_{Zn}-P_{2H}^{\bullet+}-C_{60}^{\bullet-}$ and $P_{Zn}^{\bullet+}-P_{2H}-C_{60}^{\bullet-}$ charge-separated states are estimated as 1.65 and 1.34 eV, respectively, above the neutral ground states.

Absorption Spectra. The absorption spectrum of triad **2** in 2-methyltetrahydrofuran solution is shown in Figure 1. Maxima corresponding to porphyrin absorption are found at 648, 597, 556, 515, 426, and 420 nm. The longest wavelength fullerene absorption maximum is observed at 705 nm and is of low amplitude compared to the maxima shown in Figure 1. For comparison, the spectra of model zinc and free base porphyrins **5** and **6** are also shown in the figure. The zinc porphyrin displays maxima at 596, 558, 520, 425, and 403 nm. Free base **6** has peaks at 648, 591, 546, 514, 482, 418, 401 (sh), and 373 nm.

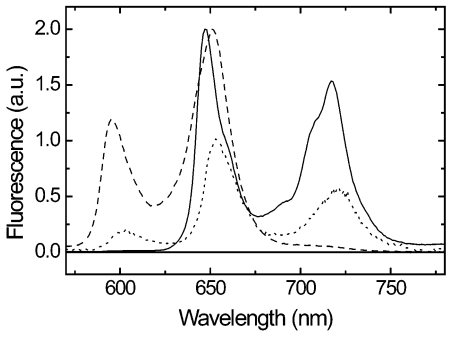

Figure 2. Fluorescence emission spectra in 2-methyltetrahydrofuran solution of triad **2** (-----), model zinc porphyrin **5** (− − −), and model free base porphyrin **6** (—), all with excitation at 423 nm. The relative fluorescence amplitudes do not represent equal absorbance at 423 nm.

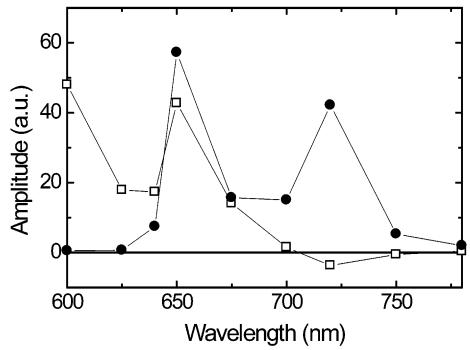

Figure 3. Decay-associated fluorescence spectra of dyad **3** in 2-methyltetrahydrofuran solution with excitation at 590 nm. Global analysis yielded two significant components with lifetimes of 58 ps (□) and 10.9 ns (●).

The spectrum of **2** differs from the sum of the spectra of model porphyrins **5** and **6** in two ways. First, the fullerene moiety contributes to the absorption throughout the spectrum from <300 nm to ~710 nm but is of high amplitude only in the 300−400 nm region. Second, in the Soret region around 420 nm, comparison of the spectrum of triad **2** with the sum of the spectra of model compounds **5** and **6** reveals excitonic splitting of 6 nm. The longer wavelength transition has the higher oscillator strength. Excitonic interactions have been observed in other porphyrin arrays.[5,7,8,13,14] There is essentially no perturbation in the Q-band region at >500 nm, where extinction coefficients are low by comparison to the Soret region; the spectrum of **2** is similar to the sum of the spectra of the model porphyrins. Dyad **3** has an absorption spectrum identical to that of **2** with the fullerene contribution absent.

The absence of excitonic interactions in the Q-band region >500 nm is expected. In the point dipole approximation, exciton theory indicates that the interaction between chromophores is inversely proportional to the cube of the interchromophoric distance and proportional to the square of the transition moments of the interacting chromophores. Thus, long-range excitonic couplings in the molecules under study are only expected for the Soret bands, which have high oscillator strengths, and not for the weaker Q-bands.[15,16]

Analysis of the absorption spectra also shows that it is possible to excite the free base porphyrin at 650 nm without exciting the zinc porphyrin and to excite the fullerene at 705 nm without exciting either porphyrin moiety. Significant, but not complete, selectivity in excitation of the zinc porphyrin may be achieved at 560 nm.

Fluorescence. The fluorescence emission spectra for **2**, **5**, and **6** in 2-methyltetrahydrofuran are shown in Figure 2. The spectra were obtained with excitation at 423 nm, where the ratio of absorption by the zinc and free base porphyrin moieties in the triad is ~65/35. The spectra of **5** and **6** have been normalized at ~650 nm for ease of comparison, and the spectrum of triad **2** is shown at a convenient amplitude. The emission of zinc porphyrin **5** shows maxima at 596 and 651 nm, whereas the free base porphyrin **6** has maxima at 648 and 717 nm. The spectrum of triad **2** features maxima at 603, 653, and 721 nm, indicating contributions from both the zinc and the free base porphyrin. The emission of both porphyrin moieties of **2** is strongly quenched relative to those of the porphyrin model systems. The free base porphyrin quenching is also observed in porphyrin−fullerene dyad **4**, but not in porphyrin dyad **3**, and is ascribed to photoinduced electron transfer to the fullerene to form a $P_{Zn}-P_{2H}^{\bullet+}-C_{60}^{\bullet-}$ charge−separated state (vide infra). The zinc porphyrin fluorescence quenching is due to singlet−singlet energy transfer to the free base porphyrin and is also observed in dyad **3**.

Time-Resolved Fluorescence. Quantitative evaluation of fluorescence quenching in **2** based on the steady-state results is not reliable, as the high degree of quenching renders the data susceptible to trace amounts of strongly emitting porphyrin impurities. Time-resolved studies using the time-correlated single photon counting technique were employed to obviate this problem and obtain kinetic data. Measurements were carried out in 2-methyltetrahydrofuran with excitation at 590 nm. Model zinc and free base porphyrins **5** and **6** yielded single-exponential fluorescence decays of 2.5 ns (goodness-of-fit parameter $\chi^2 = 1.13$) and 10.9 ns ($\chi^2 = 1.10$), respectively. The fluorescence from model porphyrin dyad **3** was measured at nine wavelengths in the 600−800 nm region. Global analysis of these data ($\chi^2 = 1.11$) yielded two significant exponential decay components with lifetimes of 58 ps and 10.9 ns (Figure 3). The 58 ps component shows positive amplitude at 600 nm, where the free base porphyrin does not emit, and is therefore associated with the decay of the zinc porphyrin first excited singlet state. This component also shows negative amplitude (a rise in emission intensity with time after the laser pulse) at 720 nm, where most of the emission comes from the free base porphyrin. This behavior demonstrates that singlet−singlet excitation energy transfer from the zinc porphyrin moiety to the free base occurs. The zinc porphyrin, therefore, acts as a light-absorbing antenna for the free base. The 10.9 ns component is due to decay of the free base porphyrin first excited singlet state. This lifetime is the same as the excited singlet state lifetime measured for model porphyrin **6**, indicating that neither energy transfer to the zinc porphyrin nor electron transfer from that moiety occurs in $P_{Zn}-{}^1P_{2H}$.

Time-resolved fluorescence experiments were also carried out for model $P_{2H}-C_{60}$ dyad **4**, and the results have been reported previously.[7] The dyad was dissolved in 2-methyltetrahydrofuran, and excitation was at 560 nm. The fluorescence was monitored at eight wavelengths in the 600−800 nm region. Global analysis of these data ($\chi^2 = 1.11$) yielded one significant decay component with a lifetime of 25 ps and three minor (≤ 5% of the decay) components with lifetimes of 0.20, 2.0, and 10 ns, which are attributed to small amounts of impurity. The significant shortening of the lifetime of $^1P_{2H}-C_{60}$ relative to that of model porphyrin **6** is ascribed to photoinduced electron transfer from the porphyrin to the fullerene to yield a $P_{2H}^{\bullet+}-C_{60}^{\bullet-}$ charge-separated state. There was no evidence for significant singlet−singlet energy transfer from the porphyrin to the fullerene, as no corresponding rise of fullerene fluorescence in the 800 nm region was observed.

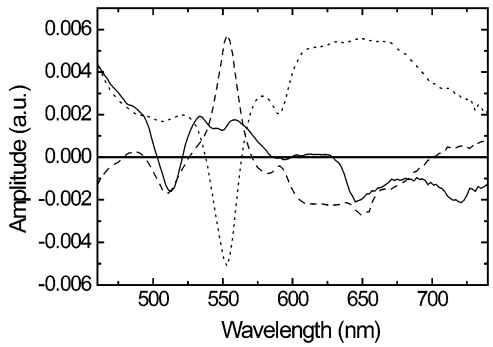

Figure 4. Decay-associated transient absorption spectra for triad **2** in 2-methyltetrahydrofuran obtained from a global analysis of transient absorption data taken after excitation at 650 nm with a ∼100 fs laser pulse. The lifetimes of the components are 25 ps (—), 157 ps (− − −), and nondecaying on this time scale (···).

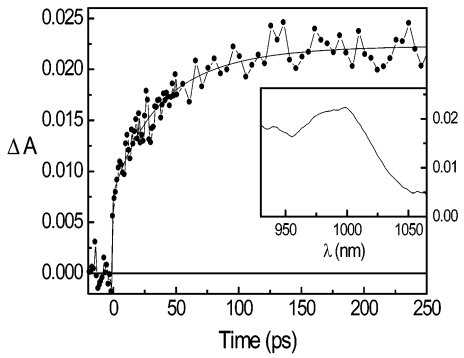

Figure 5. Transient absorption at 1000 nm measured for triad **2** with excitation at 560 nm. A three-exponential fit to the data with time constants of 25 and 57 ps, and a nondecaying component is shown as a smooth curve. The inset shows the transient absorption spectrum measured 500 ps after excitation.

Transient Absorbance. Transient absorbance measurements were performed in order to complement the results of the fluorescence studies and to allow detection of nonemissive states.

P_{Zn}−C_{60} Dyad 4. As previously reported,[7] a solution of **4** in 2-methyltetrahydrofuran was excited at 650 nm, where most of the light is absorbed by the porphyrin, with a ∼100 fs laser pulse, and the transient absorbance was monitored using a probe pulse. The spectra revealed that the porphyrin first excited singlet state decayed with a lifetime of 25 ps, consistent with the results of the fluorescence experiments. A new transient absorption grew in with the same time constant. It features absorbance in the 1000-nm region, characteristic of the fullerene radical anion, and absorbance characteristic of the porphyrin radical cation in the visible region.[17] Thus, $^1P_{2H}$−C_{60} decays by photoinduced electron transfer to yield the $P_{2H}^{\bullet+}$−$C_{60}^{\bullet-}$ charge-separated state. This state decayed to the ground state with a time constant of 3.0 ns. Similar experiments were carried out with excitation at 705 nm, where only the fullerene moiety absorbs significantly. In this case, formation of $P_{2H}^{\bullet+}$−$C_{60}^{\bullet-}$ was also observed, but the time constant was 75 ps. The lifetime of $P_{2H}^{\bullet+}$−$C_{60}^{\bullet-}$ was again found to be 3.0 ns. The fact that a 75 ps rise time for $P_{2H}^{\bullet+}$−$C_{60}^{\bullet-}$ was not observed with 650 nm excitation confirms that $^1P_{2H}$−C_{60} decays mainly by photoinduced electron transfer, rather than singlet−singlet energy transfer to the fullerene, followed by photoinduced electron transfer.

P_{Zn}−P_{2H}−C_{60} Triad 2. Triad **2** in 2-methyltetrahydrofuran was excited at 650 nm with ∼100 fs laser pulses, and the transient absorption was recorded. Excitation at this wavelength excites the free base porphyrin, but not the zinc porphyrin moiety. The spectra were measured in the 455−745 nm region (Figure 4). The best kinetic fit to the data was achieved using three exponential components, one of which did not decay during the time of the measurement (∼5 ns). The other two components have lifetimes of 25 and 157 ps. The 25 ps component has minima at about 515, 550, 590, and 650 nm that represent depletion of the free base porphyrin ground state. The negative amplitude in the region of porphyrin stimulated emission at about 650 and 720 nm indicates that the free base porphyrin first excited singlet state decays with this 25 ps lifetime, and the transient absorbance that is growing in is characteristic of the free base porphyrin radical cation. This lifetime corresponds to the decay of P_{Zn}−$^1P_{2H}$−C_{60} to form P_{Zn}−$P_{2H}^{\bullet+}$−$C_{60}^{\bullet-}$, as is also seen in the time-resolved fluorescence data.

Both the zinc porphyrin and free base porphyrin radical cations have broad absorption in the visible spectral region, but they may be distinguished by examining changes in the Q-band spectral features resulting from depletion of the ground states. The spectrum of the 157 ps component has negative amplitude in the 515 and 650 nm regions. These features are characteristic of the free base porphyrin ground state, but not the zinc porphyrin ground state, and their negative amplitude shows that they are decaying to a new species that does not have such absorbance. The spectrum also features positive amplitude around 560 nm, a wavelength where the zinc porphyrin absorbs, and represents the 157 ps rise of a transient species associated with that porphyrin. Thus, the 157 ps component is assigned to charge shift from the free base porphyrin of P_{Zn}−$P_{2H}^{\bullet+}$−$C_{60}^{\bullet-}$ to the zinc porphyrin, leading to $P_{Zn}^{\bullet+}$−P_{2H}−$C_{60}^{\bullet-}$.

The nondecaying component in Figure 4 is characteristic of the zinc porphyrin radical cation, with features due to ground-state bleaching in the 550−560 and 600 nm regions, and broad absorption in the 600−750 nm region. Thus, $P_{Zn}^{\bullet+}$−P_{2H}−$C_{60}^{\bullet-}$ does not decay on the 4 ns time scale.

The transient absorption of the solution of **2** was also studied in the 900−1100 nm spectral region, where the fullerene radical anion has a maximum.[18,19] In this case, excitation was at 560 nm. Although both porphyrin moieties absorb at this wavelength, the zinc porphyrin absorbs the majority of the light. As shown in the inset in Figure 5, excitation at this wavelength leads to formation of the fullerene radical anion, with an absorption maximum at ∼1000 nm. When the time course of the transient is monitored at 1000 nm, the radical anion absorption is seen to grow in with two time constants: 25 ps (38%) and 57 ps (62%) (Figure 5). The 25 ps rise time is ascribed to photoinduced electron transfer from P_{Zn}−$^1P_{2H}$−C_{60} to yield P_{Zn}−$P_{2H}^{\bullet+}$−$C_{60}^{\bullet-}$. The 57 ps component corresponds to the decay time of $^1P_{Zn}$−P−C_{60} and formation time of P_{Zn}−^1P−C_{60} by singlet−singlet energy transfer. Note that the lifetime of $^1P_{Zn}$−P−C_{60} is the same as that of $^1P_{Zn}$−P in dyad **3** (58 ps) within experimental error, indicating that linking the fullerene to the free base porphyrin does not open up any new decay pathways for the zinc porphyrin first excited singlet state.

Decay of the Charge-Separated State. Transient absorption spectroscopy on the nanosecond time scale was used to determine the decay characteristics of $P_{Zn}^{\bullet+}$−P_{2H}−$C_{60}^{\bullet-}$. The 2-methyltetrahydrofuran solution of **2** was excited at 590 nm with a ∼5 ns laser pulse, and the kinetics were measured at wavelengths throughout the visible and near-IR regions. The kinetic responses at 1000, 800, 560, 520, and 450 nm are shown in Figure 6. All of these responses could be satisfactorily fit with combinations of two lifetimes: 50 ns and a component that did not decay on this time scale. Experiments on a longer

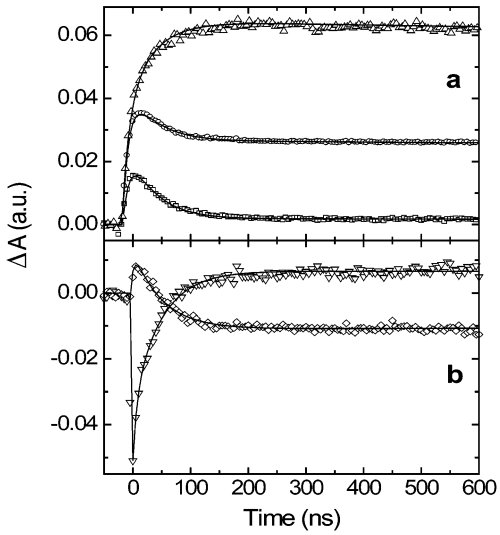

Figure 6. Transient absorption kinetics measured for triad **2** in 2-methyltetrahydrofuran at (a) 1000 nm (□), 800 nm (○), and 450 nm (△), and (b) 560 nm (▽) and 520 (◇), following excitation at 590 nm. A two-exponential fit to the data with time constants of 50 ns and several tens of μs are shown as smooth curves.

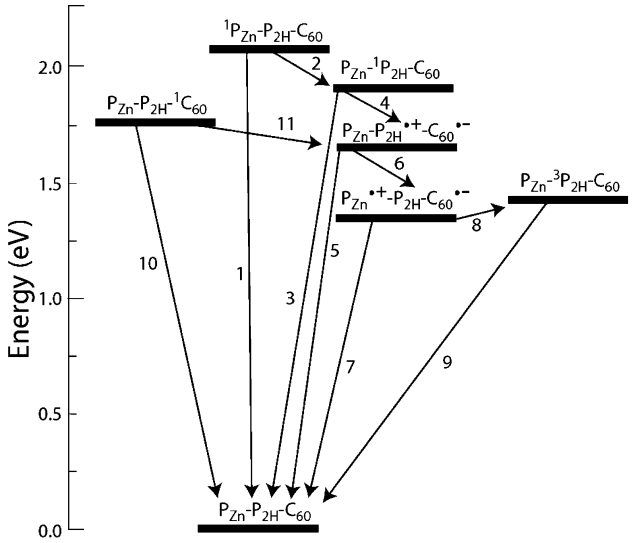

Figure 7. Transient states of $P_{Zn}-P_{2H}-C_{60}$ triad **2** and relevant interconversion pathways.

time scale showed that the nondecaying component has a lifetime of tens of microseconds, which is sensitive to the presence of oxygen. The 50 ns component was not oxygen sensitive. The long-lived component is assigned to one or more of the triplet states of **2**. The spectra at 450 and 520 nm are mainly due to the triplets and show their formation with a time constant of 50 ns. The decay at 1000 nm tracks the 50 ns disappearance of the fullerene radical anion absorbance and concomitant rise of the triplet absorbance. The zinc porphyrin radical cation absorbance at 560 and 800 nm also decays in 50 ns to produce the long-lived triplet species.

Charge recombination of $P_{Zn}^{\bullet+}-P_{2H}-C_{60}^{\bullet-}$ was also studied in benzonitrile. The decay occurred with a time constant of 220 ns, and only the molecular ground state was produced.

Discussion

Interpretation of the Kinetic Data. The model chosen for interpretation of the spectroscopic results is shown in Figure 7. The energies of the various charge-separated states were estimated from the cyclic voltammetric data presented earlier and are not corrected for any Coulombic effects. The energies of the excited singlet states of the zinc porphyrin (2.08 eV), free base porphyrin (1.91 eV), and fullerene (1.75 eV) moieties were calculated from the wavenumber average of the longest wavelength absorption maximum and shortest wavelength emission maximum of model compounds. Each of the various possible interconversions indicated in the Figure (e.g., step 1) has associated with it a corresponding rate constant (e.g., k_1). Values for some of the rate constants for triad **2** may be estimated using the values obtained from the model compounds. Below, we will discuss these processes, and then turn to the triad itself.

Porphyrins 5 and 6 and Fullerene. The time-resolved fluorescence data show that the excited singlet state of zinc porphyrin **5** decays with a time constant of 2.5 ns, which is typical for zinc porphyrins of this general type. Similarly, the 10.9 ns lifetime found for the first excited singlet state of free base porphyrin **6** is typical for such porphyrins. On the basis of these numbers, we estimate values for k_1 and k_3 in Figure 7 of 4.0×10^8 and 9.2×10^7 s^{-1}, respectively. Substituted fullerenes with structures similar to that in **2** and **4** have an excited singlet state lifetime of 1.4 ns,[20] and this time constant is used to assign a value of 7.1×10^8 s^{-1} for k_{10}.

$P_{2H}-C_{60}$ Dyad 4. The lifetime of $^1P_{2H}-C_{60}$ is dramatically shortened via electron transfer to the fullerene to yield $P_{2H}^{\bullet+}-C_{60}^{\bullet-}$. The rate constant for photoinduced electron transfer, k_{ET}, may be calculated from eq 1

$$1/\tau_s = k_{ET} + k_3 \qquad (1)$$

where τ_s is the 25-ps lifetime of $^1P_{2H}-C_{60}$ found in both the time-resolved fluorescence and transient absorbance studies and equals 4.0×10^{10} s^{-1}. The quantum yield of $P_{2H}^{\bullet+}-C_{60}^{\bullet-}$ is 1.0. The rate constant for charge recombination, k_{CR}, is the reciprocal of the 3.0 ns lifetime observed by transient absorption and equals 3.3×10^8 s^{-1}.

With excitation at 705 nm, the fullerene first excited singlet state, $P_{2H}-^1C_{60}$, was produced. The lifetime of this state, 75 ps, is substantially quenched due to photoinduced electron transfer to yield $P_{2H}^{\bullet+}-C_{60}^{\bullet-}$, as demonstrated by the time-resolved absorption experiments. Using an equation similar to eq 1 and the rate constant for decay of the unperturbed fullerene first excited singlet state given above, the rate constant for photoinduced electron transfer from $P_{2H}-^1C_{60}$ is 1.3×10^{10} s^{-1}. The quantum yield of $P_{2H}^{\bullet+}-C_{60}^{\bullet-}$ formed by this route is 0.95. We assume that k_{11} in Figure 7 also equals 1.3×10^{10} s^{-1}, although this state was not populated significantly during the study of triad **2**.

$P_{Zn}-P_{2H}$ Dyad 3. The fluorescence results for **3** show that linking the zinc porphyrin to the free base does not perturb the decay kinetics of the free base porphyrin, consistent with our assignment of k_3 as 9.2×10^7 s^{-1}. The lifetime of the zinc porphyrin first excited singlet state is quenched from 2.5 ns to only 58 ps in the dyad, due to singlet−singlet energy transfer to the free base to form $P_{Zn}-^1P_{2H}$. The occurrence of singlet energy transfer is demonstrated by the rise of free base fluorescence emission that accompanies the decay of zinc porphyrin emission. In principle, photoinduced electron transfer from the zinc porphyrin first excited singlet state to form $P_{Zn}^{\bullet+}-P_{2H}^{\bullet-}$ could also contribute to the relaxation of $^1P_{Zn}-P_{2H}$. However, the thermodynamic driving force for electron transfer is small. No evidence for formation of the zinc porphyrin radical cation with a 58 ps time constant was obtained from the

time-resolved absorption studies of triad **2**. Thus, the rate constant for singlet−singlet energy transfer is taken as $(1/58 \times 10^{-12}\ s) - k_1$, or $1.7 \times 10^{10}\ s^{-1}$. On this basis, the quantum yield of singlet−singlet energy transfer in **3** is 0.98.

P_{Zn}−P_{2H}−C_{60} Triad 2. When **2** was excited at 650 nm to generate P_{Zn}−$^1P_{2H}$−C_{60}, the porphyrin first excited state was found to decay with a time constant of 25 ps to yield P_{Zn}−$P_{2H}^{\bullet+}$−$C_{60}^{\bullet-}$. This behavior is identical to that observed for P_{2H}−C_{60} dyad **4** and yields a value for k_4 in Figure 7 of $4.0 \times 10^{10}\ s^{-1}$. The quantum yield of charge separation from the free base porphyrin excited state is 1.0. The transient absorbance results for **2** demonstrate that P_{Zn}−$P_{2H}^{\bullet+}$−$C_{60}^{\bullet-}$ is converted into $P_{Zn}^{\bullet+}$−P_{2H}−$C_{60}^{\bullet-}$ with a time constant of 157 ps via charge shift reaction step 6. If we assume that charge recombination of P_{Zn}−$P_{2H}^{\bullet+}$−$C_{60}^{\bullet-}$ occurs with the same time constant that it does in dyad **4** (3.0 ns), then $k_5 = 3.3 \times 10^8\ s^{-1}$. Thus, the charge-shift reaction occurs with $k_6 = (1/157 \times 10^{-12}\ s) - k_5$, or $6.0 \times 10^9\ s^{-1}$. The overall quantum yield of $P_{Zn}^{\bullet+}$−P_{2H}−$C_{60}^{\bullet-}$ produced from P_{Zn}−$^1P_{2H}$−C_{60} is 0.95. As electron transfer requires some form of orbital overlap between donor and acceptor, the relatively rapid charge-shift reaction must involve superexchange through the aryl groups joining the two porphyrin moieties, with a possible contribution from "through-space" electron transfer via direct overlap of the two porphyrin π-electron systems.[21]

When **2** is excited at 560 nm, where both the zinc and free base porphyrins absorb, the formation of the initial P_{Zn}−$P_{2H}^{\bullet+}$−$C_{60}^{\bullet-}$ state occurs with two time constants: 25 and 57 ps. The first time constant corresponds to formation of P_{Zn}−$P_{2H}^{\bullet+}$−$C_{60}^{\bullet-}$ from P_{Zn}−$^1P_{2H}$−C_{60} formed by direct excitation, as discussed above. The second lifetime is identical to the lifetime of $^1P_{Zn}$−P in dyad **3**, within experimental error, and is associated with singlet−singlet energy transfer from the zinc porphyrin to the free base. Thus, in the triad, singlet−singlet energy transfer from the zinc porphyrin to the free base (step 2 in Figure 7) occurs with $k_2 = 1.7 \times 10^{10}\ s^{-1}$. This is followed by photoinduced electron transfer to the fullerene (step 4) to give P_{Zn}−$P_{2H}^{\bullet+}$−$C_{60}^{\bullet-}$. Because $k_4 > k_2$, the charge-separated state forms with the time constant for energy transfer. The correspondence of the lifetime of $^1P_{Zn}$−P_{2H}−C_{60} in the triad with that of $^1P_{Zn}$−P_{2H} in dyad **3** shows that direct photoinduced electron transfer from the zinc porphyrin to the fullerene is much slower than singlet energy transfer from the zinc to free base porphyrins and is not observed. As mentioned above, photoinduced electron transfer from the zinc porphyrin first excited singlet state to the free base porphyrin is thermodynamically possible, but no evidence for the competition of this process with energy transfer was observed.

Charge recombination of $P_{Zn}^{\bullet+}$−P_{2H}−$C_{60}^{\bullet-}$ occurs with a time constant of 50 ns, and formation of triplet states is observed. Assuming that there is no recombination directly to the ground state (vide infra), the charge recombination rate constant k_8 equals $2.0 \times 10^7\ s^{-1}$. The energy of the lowest triplet state of a model for the fullerene moiety of **2** is 1.50 eV.[22] Although the triplet state energies of the porphyrin moieties of **2** have not been measured, similar zinc and free base porphyrin triplet states have energies of 1.55 and 1.43 eV above the ground state, respectively.[23] Because P_{Zn}−$^3P_{2H}$−C_{60} is the lowest energy triplet state in the molecule, Figure 7 shows this state as the charge recombination product. The distribution of energy among the three triplet states in the triad at various times after formation is not known. In benzonitrile, charge recombination occurs in 220 ns ($k_7 = 4.5 \times 10^6\ s^{-1}$) to yield only the molecular ground state.

TABLE 1: Rate Constants and Quantum Yields for Photochemical Processes in Triad 2 Dissolved in 2-Methyltetrahydrofuran

reaction[a]	rate constant (s^{-1})	% yield[b]	reaction[a]	rate constant (s^{-1})	% yield[b]
step 1	4.0×10^8		step 7[c]	$<4.5 \times 10^6$	<22
step 2	1.7×10^{10}	98	step 8[c]	$>1.6 \times 10^7$	>78
step 3	9.2×10^7		step 9	$<1 \times 10^5$	
step 4	4.0×10^{10}	100	step 10	7.1×10^8	
step 5	3.3×10^8	5	step 11	1.3×10^{10}	95
step 6	6.0×10^9	95			

[a] See Figure 7. [b] Yield based on indicated step only. [c] See discussion in the text.

As shown above, it is possible to use the data obtained for triad **2** and the related model compounds to extract values for all 11 rate constants in Figure 7. For convenience, these are collected in Table 1.

Singlet−Singlet Energy Transfer. The singlet−singlet energy transfer rate constant k_2 found for transfer from the zinc porphyrin first excited singlet state to the free base porphyrin in triad **2** and the identical value for dyad **3** ($1.7 \times 10^{10}\ s^{-1}$) is large enough to ensure that the zinc porphyrin moiety is a good antenna for the free base porphyrin energy trap state ($\Phi_2 = 98\%$). The transfer rate is identical to the rate constant for singlet energy transfer between zinc porphyrin moieties estimated for hexad **1** using fluorescence anisotropy techniques.[5] The energy transfer could occur by the Förster dipole−dipole mechanism,[24,25] or through-bond, electron-exchange-mediated (Dexter-type) coupling might also contribute, as has been demonstrated in other porphyrin arrays.[13,14,26,27] Although the linkage joining the chromophores consists of three phenyl rings, these have dihedral angles in the range of ~60°−90° to one another and to the porphyrin π-electron systems, which reduces electronic overlap. The spatial separation between the two porphyrins is relatively small, and significant direct overlap of the π-electron systems that could enable electron-exchange-mediated transfer could be present. The occurrence of electron transfer between the porphyrins at reasonably high rates demonstrates that significant electronic exchange interaction is present, and so energy transfer by that process cannot be ignored a priori.

The theoretical transfer rate by the dipole−dipole mechanism, k_{DD}, was estimated using Förster's eq 2

$$k_{DD} = \frac{0.529\kappa^2\Phi_{f_D}}{n^4 N \tau_D R^6} \int f_D(\nu)\epsilon_A(\nu)\nu^{-4}\,d\nu \qquad (2)$$

where κ is an orientation factor, Φ_{f_D} is the fluorescence quantum yield of the donor chromophore, n is the index of refraction of the medium, N is Avogadro's number, τ_D is the lifetime of the donor first excited singlet state, R is the separation of the dipoles, and ν is the frequency. The integral is the overlap of the normalized donor fluorescence emission spectrum and the absorbance spectrum of the acceptor. Molecular mechanics modeling of dyad **3** (MM2) yields $R = 10.6$ Å for the distance between the centers of the porphyrin rings. Each porphyrin plane is tilted at an angle of 39° with respect to the plane of the central benzene core. The value of the orientation factor κ^2 depends on the choice of transition dipoles and the location of the central hydrogen atoms in the free base porphyrin. The average value for κ^2 based on the various dipole−dipole orientations in the energy-minimized structure is 1.0. Using these data and reported values for the photophysical parameters of zinc 5,10,15,20-

tetrakis(2,4,6-trimethylphenyl)porphyrin and its free base analogue[28−30] and the 2.5 ns value for τ_D found for **5**, a singlet−singlet energy transfer rate constant of 2.5×10^{10} s^{-1} is calculated. This is very close to the observed value of 1.7×10^{10} s^{-1}, demonstrating that singlet−singlet energy transfer in **2** and **3** can be readily explained by the dipole−dipole mechanism. The calculated energy transfer rate constant is larger for **2** and **3** than for a similar structure with two zinc porphyrin moieties (such as **1**) because of more favorable overlap of the donor emission and acceptor absorbance spectra.

Electron Transfer. Photoinduced electron transfer from the free base porphyrin first excited singlet state to the fullerene is very rapid, and charge recombination is relatively slow. Incorporating the $P_{2H}-C_{60}$ unit into the multiple ring system containing the zinc porphyrin does not affect the rates and yields of the photoinduced electron transfer, as the rate constants are the same for **2** and $P_{2H}-C_{60}$ dyad **4**. Thus, future expansion of the supermolecular system to include additional antenna pigments is unlikely to interfere with photoinduced electron transfer.

Charge shift from the zinc porphyrin to the free base porphyrin radical cation in $P_{Zn}-P_{2H}^{\bullet+}-C_{60}^{\bullet-}$ is much more rapid than charge recombination of the intermediate (Table 1), ensuring a high yield of the final $P_{Zn}^{\bullet+}-P_{2H}-C_{60}^{\bullet-}$ state (95%). This is important to the useful operation of the molecule, because moving the positive charge away from the radical anion reduces electronic coupling and increases the lifetime of the charge-separated state.

The charge shift reaction requires electronic orbital overlap between the two porphyrin moieties. This could in principle be through "space" by direct overlap of the π-orbitals of the two moieties or via superexchange involving the bonds of the aryl linkers. The results obtained here do not reveal the relative contributions of these two mechanisms. However, the rate constant for the charge shift reaction in **2** is only 2.6 times larger than that for a charge shift of similar driving force from a zinc porphyrin to a free base porphyrin radical cation linked via a diarylacetylene bridge.[7] In the latter system, the geometry suggests that the transfer must occur via the linkage bonds.

Charge Recombination. In 2-methyltetrahydrofuran, charge recombination yields a triplet state, rather than the ground state of triad **2**. Although charge recombination to give triplets occurs in natural photosynthesis, it was first observed in porphyrin-based model systems only recently.[31] Such recombination has now been found in a number of porphyrin−fullerene constructs.[20,32−35] Facile recombination to energetically accessible triplet states is due to the long lifetime of the charge-separated state combined with the weak electronic coupling of the radical ions, which allows spin equilibration in the biradical prior to recombination.

Recombination of this type is somewhat unexpected in **2** because the three relevant triplet states, $^3P_{Zn}-P_{2H}-C_{60}$, $P_{Zn}-{}^3P_{2H}-C_{60}$, and $P_{Zn}-P_{2H}-{}^3C_{60}$, are estimated to lie 1.55, 1.43, and 1.50 eV above the ground state, whereas the energy of the $P_{Zn}^{\bullet+}-P_{2H}-C_{60}^{\bullet-}$ charge-separated state is estimated as 1.34 eV. Although these estimates are based on model systems and therefore subject to some uncertainty, they suggest that the recombination reaction must be endergonic, or nearly so. Variable temperature studies to investigate this question have not yet been carried out, but there is ample thermal energy at ambient temperatures to allow endergonic charge recombination to the fullerene or porphyrin triplet states. The initial and final triplet states resulting from charge recombination are as yet unknown, and thermally driven equilibration among porphyrin and fullerene triplet states has been observed in molecules of this general type.[36]

There are in principle several recombination mechanisms that satisfy thermodynamic constraints. The $P_{Zn}^{\bullet+}-P_{2H}-C_{60}^{\bullet-}$ state could undergo endergonic electron-transfer back to $P_{Zn}-P_{2H}^{\bullet+}-C_{60}^{\bullet-}$ and a resulting triplet biradical could recombine to give a porphyrin or fullerene triplet state. Charge recombination by a two-step mechanism has been observed in other porphyrin-based donor−acceptor systems.[37−39] Alternatively, $P_{Zn}^{\bullet+}-P_{2H}-C_{60}^{\bullet-}$ could recombine directly to give one or more of the available triplets, which could then equilibrate so as to populate mainly the lowest lying triplet, $P_{ZN}-{}^3P_{2H}-C_{60}$. Additional studies will be necessary to unravel this situation.

Yield of the Recombination Triplet. In benzonitrile, the lifetime of $P_{Zn}^{\bullet+}-P_{2H}-C_{60}^{\bullet-}$ is much longer than in 2-methyltetrahydrofuran, and recombination yields only the molecular ground state. The change in mechanism can be qualitatively understood in terms of the Marcus−Hush theory for electron transfer.[40−43] It is well-known that fullerenes and porphyrins have relatively low total reorganization energies for electron transfer (λ), compared to more traditional electron acceptors such as quinones.[31,32,44−47] A consequence of this is that in relatively nonpolar solvents such as 2-methyltetrahydrofuran, charge recombination to the ground state, which is strongly exergonic, lies in the inverted region of the Marcus−Hush relationship of electron-transfer rate constant and thermodynamic driving force ($\Delta G°$). The driving force for charge recombination to a triplet state, however, is much less, and the reaction almost certainly lies in the normal region of the relationship, and happens to be faster than recombination to the ground state. Charge recombination to the ground state is retarded, whereas recombination to a triplet is facile and dominates the relaxation process. In a polar solvent such as benzonitrile, however, the charge-separated state is stabilized by interaction with solvent dipoles, and this reduces the driving force for ground-state recombination and adds to the energetic barrier in the two-step, exergonic triplet recombination. Direct, endergonic recombination to a triplet would also be slowed by solvent stabilization of the charge-separated state. In addition, the solvent reorganization energy increases in the more polar solvent, shifting the maximum of the Marcus−Hush relationship in the direction of increasing driving force. The result of both effects is to shift the recombination to the ground state (inverted region) toward the maximum of the curve where $-\Delta G° = \lambda$ (faster rate) and to shift the recombination to the triplet state away from the maximum (slower rate). The net result is the observed switchover of mechanisms.

The yield of triplet states by recombination step 8 in Figure 7 or the alternative two-step process was not measured, but it is possible to put limits on the values of k_7 and the rate constant for triplet formation, k_{tr}, regardless of the exact mechanism for triplet formation. In benzonitrile, recombination yields only the ground state, and $k_7 = 4.5 \times 10^6$ s^{-1}. In 2-methyltetrahydrofuran, k_7 will necessarily be less than this, for the reasons mentioned above. In 2-methyltetrahydrofuran, $k_7 + k_{tr} = 2.0 \times 10^7$ s^{-1}. Thus, $k_{tr} > 1.6 \times 10^7$ s^{-1}, and the yield of triplet states is >78%.

Conclusions

A convenient and flexible method for the synthesis of the hexaarylbenzene framework bearing porphyrin moieties has been developed. Unlike previously reported methods, this one allows facile preparation of nonsymmetrical structures wherein various antenna moieties and electron-transfer components may be

linked to the same hexaphenylbenzene core. Triad **2** demonstrates rapid singlet−singlet energy transfer from the zinc porphyrin to the free base porphyrin energy trap, followed by fast photoinduced electron transfer to form a $P_{Zn}-P_{2H}^{\bullet+}-C_{60}^{\bullet-}$ charge-separated state. The same state is formed by direct excitation of the free base porphyrin or fullerene moieties. Thus, light at any wavelength from <300 nm to ~710 nm initiates formation of the charge-separated state. Electron transfer from the zinc porphyrin yields a final $P_{Zn}^{\bullet+}-P_{2H}-C_{60}^{\bullet-}$ charge-separated state having a lifetime of 50 ns in 2-methyltetrahydrofuran, with recombination to give triplet states, or 220 ns in benzonitrile, with recombination to the ground state. Although the yield of the long-lived charge-separated state depends slightly on the excitation wavelength, it is >90% throughout the absorbance spectrum. This molecular system is therefore suitable for elaboration into more complex "supermolecular" systems with interesting energy and electron-transfer properties.

Experimental Section

Synthesis. The preparations of porphyrins **5**[48] and **6**[49] and porphyrin−fullerene dyad **4**[7] have been previously reported.

5-(4-Carboxymethylphenyl)-15-{4-[2-(triisopropylsilyl)-ethynyl]phenyl}-10,20-bis(2,4,6-trimethylphenyl)porphyrin (7). A heavy-walled glass tube charged with 200 mg (0.227 mmol) of 5-(4-carboxymethylphenyl)-15-(4-iodophenyl)-10,20-bis(2,4,6-trimethylphenyl)porphyrin,[7] triethylamine (50 mL), and 112 mg (0.363 mmol) of triphenylarsine was cooled to 0 °C, and the contents were flushed with argon for 15 min. Triisopropylsilylacetylene (100 μL, 0.453 mmol) and 40 mg (0.045 mmol) of tris(dibenzylideneacetone)palladium(0) were added and flushing with argon was continued for an additional 10 min. The tube was sealed with a Teflon screw stopper and the reaction mixture was warmed to 40 °C for 24 h. The solvent was evaporated and the residue was chromatographed on silica gel (dichloromethane/hexanes, 1:1) to give 166 mg (78% yield) of porphyrin (**7**): ^{1}H NMR (300 MHz, $CDCl_3$) δ −2.63 (2H, s, N−H), 1.25 (21H, s, ^{i}Pr-H), 1.84 (12H, s, Ar−CH_3), 2.63 (6H, s, Ar−CH_3), 4.10 (3H, s, $COOCH_3$), 7.28 (4H, s, Ar−H), 7.87 (2H, d, J = 7 Hz, Ar−H), 8.17 (2H, d, J = 7 Hz, Ar−H), 8.31 (2H, d, J = 8 Hz, Ar−H), 8.42 (2H, d, J = 8 Hz, Ar−H), 8.65−8.80 (8H, m, β-H); MS *m*/*z* calcd for $C_{61}H_{64}N_4O_2Si$ 937, obsd 937; UV/vis (dichloromethane) 422, 516, 552, 592, 648 nm.

5-(4-Carboxymethylphenyl)-15-(4-ethynylphenyl)-10,20-bis(2,4,6-trimethylphenyl)porphyrin (8). To a flask containing 100 mg (0.107 mmol) of porphyrin **7** and 20 mL of tetrahydrofuran was added 0.3 g of tetrabutylamonium fluoride/silica gel (0.1 equiv/g), and the suspension was stirred under a nitrogen atmosphere for 30 min. The solid material was removed by filtration and the filtrate was concentrated by evaporation at reduced pressure. The residue was chromatographed on silica gel (dichloromethane/hexanes 1:1) to give 74 mg (89% yield) of the expected porphyrin **8**: ^{1}H NMR (300 MHz, $CDCl_3$) δ −2.64 (2H, s, N−H), 1.83 (12H, s, Ar−CH_3), 2.62 (6H, s, Ar−CH_3), 3.31 (1H, s, ≡C−H), 4.10 (3H, s, $COOCH_3$), 7.28 (4H, s, Ar−H), 7.88 (2H, d, J = 8 Hz, Ar−H), 8.19 (2H, d, J = 8 Hz, Ar−H), 8.31 (2H, d, J = 8 Hz, Ar−H), 8.43 (2H, d, J = 8 Hz, Ar−H), 8.70−8.79 (8H, m, β-H); MS *m*/*z* calcd for $C_{54}H_{44}N_4O_2$ 781, obsd 781; UV/vis (dichloromethane) 420, 516, 552, 592, 650 nm.

1-{4-[10-(4-Carboxymethylphenyl)-15,20-bis(2,4,6-trimethylphenyl)porphyrin-5-yl]phenyl}-2-{4-[10,15,20-tris(2,4,6-trimethylphenyl)porphyrin-5-yl-(zinc complex)]phenyl}ethyne (9). A threaded tube containing 100 mg (0.128 mmol) of porphyrin **8**, 119 mg (0.128 mmol) of 5-(4-iodophenyl)-10,15,20-tris(2,4,6-trimethyphenyl)porphyrin, zinc complex (prepared by treating the free base[49] with zinc acetate), 63 mg (0.21 mmol) of triphenylarsine, and 30 mL of triethylamine was cooled and flushed with argon for 20 min. Tris(dibenzylideneacetone)-palladium(0) (23 mg, 0.026 mmol) was added to the reaction mixture and flushing with argon was continued for an additional 10 min. The tube was then sealed with a threaded stopper. After 24 h at 40 °C, the solvent was evaporated, the residue redissolved in dichloromethane/hexanes (1:1) plus several drops of pyridine, and the mixture chromatographed on silica gel (dichloromethane/hexanes 1:1 to 2:1) to give 112 mg (69% yield) of **9**: ^{1}H NMR (300 MHz, $CDCl_3$) δ −2.60 (2H, s, N−H), 1.79 (6H, s, Ar−CH_3), 1.84 (12H, s, Ar−CH_3), 1.86 (12H, s, AR−CH_3), 2.62 (3H, s, Ar−CH_3), 2.63 (6H, s, Ar−CH_3), 2.64 (6H, s, Ar−CH_3), 4.11 (3H, s, $COOCH_3$), 7.28 (2H, s, Ar−H), 7.30 (4H, s, Ar−H), 7.32 (4H, s, Ar−H), 8.07 (2H, d, J = 7 Hz, Ar−H), 8.09 (2H, d, J = 8 Hz, Ar−H), 8.31 (2H, d, J = 7 Hz, Ar−H), 8.32 (2H, d, J = 8 Hz, Ar−H), 8.34 (2H, d, J = 8 Hz, Ar−H), 8.45 (2H, d, J = 8 Hz, Ar−H), 8.71−8.93 (16H, m, β-H); MS *m*/*z* calcd for $C_{107}H_{88}N_8O_2Zn$ 1583, obsd 1583; UV/vis (dichloromethane) 422, 516, 552, 592, 648 nm.

$P_{Zn}-P_{2H}$ Dyad 3. A mixture of 100 mg (0.063 mmol) of **9**, 0.240 g (0.632 mmol) of tetraphenylcyclopentadienone, and 7 mL of diphenyl ether was warmed to reflux under a nitrogen atmosphere. After 5 h the solvent was removed by distillation under vacuum and the residue was chromatographed on silica gel (dichloromethane/hexanes 1:1 to 3:2) to give 90 mg (74% yield) of **3**: ^{1}H NMR (300 MHz, $CDCl_3$) δ −2.73 (2H, s, N−H), 1.34 (6H, s, Ar−CH_3), 1.38 (6H, s, Ar−CH_3), 1.85 (6H, s, Ar−CH_3), 1.87 (12H, s, Ar−CH_3), 2.06 (3H, s, Ar−CH_3), 2.14 (3H, s, Ar−CH_3), 2.61 (3H, s, Ar−CH_3), 2.67 (6H, s, Ar−CH_3), 4.09 (3H, s, $COOCH_3$), 6.65 (2H, s, Ar−H), 6.73 (2H, s, Ar−H), 6.95−7.25 (22H, m, Ar−H), 7.32 (4H, s, Ar−H), 7.50 (2H, d, J = 6 Hz, Ar−H), 7.52 (2H, d, J = 6 Hz, Ar−H), 7.93 (2H, d, J = 2 Hz, Ar−H), 7.96 (2H, d, J = 2 Hz, Ar−H), 8.01 (1H, d, J = 4 Hz, β-H), 8.18 (1H, d, J = 5 Hz, β-H), 8.28 (2H, d, J = 8 Hz, Ar−H), 8.40 (2H, d, J = 8 Hz, Ar−H), 8.45−8.76 (14H, m, β-H); MS *m*/*z* calcd for $C_{135}H_{108}N_8O_2Zn$ 1940, obsd 1940; UV/vis (dichloromethane) 420, 516, 550, 590, 652 nm.

1-{4-[10-(4-Formylphenyl)-15,20-bis(2,4,6-trimethylphenyl)-porphyrin-5-yl]phenyl}-2-{4-[10,15,20-tris(2,4,6-trimethyl-phenyl)porphyrin-5-yl-(zinc complex)]phenyl}-3,4,5,6-tetraphenylbenzene (10). To a flask containing 90 mg (0.046 mmol) of **3** and 20 mL of tetrahydrofuran at 0 °C were added small portions of lithium aluminum hydride until the starting material had been consumed. The reaction was then quenched by adding ice and the product was extracted into dichloromethane. The solvent was evaporated and the residue was redissolved in dichloromethane (20 mL). Activated manganese dioxide was added in portions to the stirred solution until the starting material had been converted to a less polar material (reaction course followed by TLC). The solid was removed by filtration and the filtrate was concentrated by distillation under reduced pressure. The residue was chromatographed on silica gel (dichloromethane/hexanes 3:2) to give 73 mg (82% yield) of **10**: ^{1}H NMR (300 MHz, $CDCl_3$) δ −2.72 (2H, s, N−H), 1.34(6H, s, Ar−CH_3), 1.38 (6H, s, Ar−CH_3), 1.84 (6H, s, Ar−CH_3), 1.87 (12H, s, Ar−CH_3), 2.06 (3H, s, Ar−CH_3), 2.13 (3H, s, Ar−CH_3), 2.61 (3H, s, Ar−CH_3), 2.67 (6H, s, Ar−CH_3), 6.65 (2H, s, Ar−H), 6.72 (2H, s, Ar−H), 6.93−7.24 (22H, m, Ar−H), 7.32 (4H, s, Ar−H), 7.50 (2H, d, J = 7 Hz, Ar−H), 7.53 (2H, d, J = 7 Hz, Ar−H), 7.93 (2H, d, J = 2 Hz, Ar−H), 7.96 (2H, d, J = 2 Hz, Ar−H), 8.01 (1H, d, J = 5 Hz, β-H), 8.17 (1H, d,

$J = 5$ Hz, β-H), 8.25 (2H, d, $J = 8$ Hz, Ar−H), 8.39 (2H, d, $J = 8$ Hz, Ar−H), 8.49−8.76 (14H, m, β-H), 10.35 (1H, s, −CHO); MS *m/z* calcd for $C_{134}H_{106}N_8O_1Zn$ 1910, obsd 1909; UV/vis 420, 516, 552, 592, 650 nm.

P_{Zn}−P_{2H}−C_{60} Triad 2. A flask containing 60 mg (0.031 mmol) of **10**, 45 mg (0.063 mmol) of C_{60}, 28 mg (0.31 mmol) of sarcosine, and 40 mL of toluene was heated to reflux under an argon atmosphere for 20 h. The solvent was evaporated at reduced pressure and the residue was redissolved in a mixture of carbon disulfide, toluene, and hexanes (50:33:17). The resulting solution was applied to a silica gel column and eluted with toluene/hexanes (2:1 to 3:1) to give 47 mg (56% yield) of triad **2**: ^{1}H NMR (300 MHz, $CDCl_3$) δ −2.74 (2H, s, N−H), 1.32 (3H, s, Ar−CH_3), 1.34 (3H, s, Ar−CH_3), 1.38 (6H, s, Ar−CH_3), 1.84 (9H, s, Ar−CH_3), 1.86 (9H, s, Ar−CH_3), 2.05 (3H, s, Ar−CH_3), 2.12 (3H, s, Ar−CH_3), 2.61 (3H, s, Ar−CH_3), 2.66 (6H, s, Ar−CH_3), 3.10 (3H, s, N−CH_3), 4.41 (1H, d, $J = 9$ Hz, pyrrolid-H), 5.10 (1H, d, $J = 9$ Hz, pyrrolid-H), 5.26 (1H, s, pyrrolid-H), 6.63 (2H, s, Ar−H), 6.72 (2H, s, Ar−H), 6.92−7.23 (22H, m, Ar−H), 7.31 (4H, s, Ar−H), 7.49 (2H, d, $J = 8$ Hz, Ar−H), 7.51 (2H, d, $J = 8$ Hz, Ar−H), 7.92 (2H, d, $J = 4$ Hz, Ar−H), 7.95 (2H, d, $J = 4$ Hz, Ar−H), 7.99 (1H, d, $J = 5$ Hz, β-H), 8.17 (1H, d, $J = 5$ Hz, β-H), 8.10−8.22 (2H, brd s, Ar−H), 8.25 (2H, d, $J = 8$ Hz, Ar−H), 8.38−8.75 (14H, m, β-H); LR-FAB-MS *m/z* calcd for $C_{196}H_{111}N_9Zn$ 2657, obsd 2657; UV/vis (dichloromethane) 418, 518, 552, 592, 652, 704 nm.

Spectroscopic Measurements. ^{1}H NMR spectra were recorded on Varian Unity spectrometers at 300 or 500 MHz. Samples were dissolved in deuteriochloroform with tetramethylsilane as an internal reference. Mass spectra were obtained on a matrix-assisted laser desorption/ionization time-of-flight spectrometer (MALDI-TOF) or a Kratos MS 50 mass spectrometer operating at 8 eV in FAB mode. Ultraviolet−visible ground state absorption spectra were measured on a Shimadzu UV2100U spectrometer. The solvent for all optical measurements was freshly distilled 2-methyltetrahydrofuran, unless otherwise stated. All samples were deoxygenated by bubbling with argon for 20 min.

Steady-state fluorescence emission spectra were measured using a Photon Technology International MP-1 fluorometer and corrected. Excitation was produced by a 75 W xenon lamp and single grating monochromator. Fluorescence was detected at 90° to the excitation beam via a single grating monochromator and an R928 photomultiplier tube having S-20 spectral response operating in the photon counting mode.

Fluorescence decay measurements were performed on $\sim 1 \times 10^{-5}$ M solutions by the time-correlated single photon counting method. The excitation source was a cavity-dumped Coherent 700 dye laser pumped by a frequency-doubled Coherent Antares 76s Nd:YAG laser. Fluorescence emission was detected at a magic angle using a single grating monochromator and microchannel plate photomultiplier (Hamamatsu R2809U-11). The instrument response time was ca. 35−50 ps, as verified by scattering from Ludox AS-40. The spectrometer was controlled by software based on a LabView program from National Instruments.[50] Experimental uncertainties associated with the reported lifetimes were typically ≤5%.

Nanosecond transient absorption measurements were made with excitation from an Opotek optical parametric oscillator pumped by the third harmonic of a Continuum Surelight Nd:YAG laser. The pulse width was ~5 ns, and the repetition rate was 10 Hz. Experimental uncertainties associated with the reported lifetimes were typically ≤5%. The detection portion of the spectrometer has been described elsewhere.[51]

The femtosecond transient absorption apparatus consisted of a kilohertz pulsed laser source and a pump−probe optical setup. The laser pulse train was provided by a Ti:sapphire regenerative amplifier (Clark-MXR, Model CPA-1000) pumped by a diode-pumped CW solid-state laser (Spectra Physics, Model Millennia V). The typical laser pulse was 100 fs at 790 nm, with a pulse energy of 0.9 mJ at a repetition rate of 1 kHz. Most of the laser energy (80%) was used to pump an optical parametric amplifier (IR-OPA, Clark-MXR). The excitation pulse was sent through a computer-controlled optical delay line. The remaining laser output (20%) was focused into a 1.2 cm rotating quartz plate to generate a white light continuum. The continuum beam was further split into two identical parts and used as the probe and reference beams, respectively. The probe and reference signals were focused onto two separated optical fiber bundles coupled to a spectrograph (Acton Research, Model SP275). The spectra were acquired on a dual diode array detector (Princeton Instruments, Model DPDA-1024). Experimental uncertainties associated with the reported lifetimes were typically ≤5%.[52]

To determine the number of significant components in the transient absorption data, singular value decomposition analysis[53,54] was carried out using locally written software based on the MatLab 5.0 program (MathWorks, Inc.). Decay-associated spectra were then obtained by fitting the transient absorption change curves over a selected wavelength region simultaneously as described by eq 3

$$\Delta A(\lambda,t) = \sum_{i=1}^{n} A_i(\lambda) \exp(-t/\tau_i) \qquad (3)$$

where $\Delta A(\lambda,t)$ is the observed absorption change at a given wavelength at time delay t and n is the number of kinetic components used in the fitting. A plot of $A_i(\lambda)$ versus wavelength is called a decay-associated spectrum and represents the amplitude spectrum of the ith kinetic component, which has a lifetime of τ_i.

Acknowledgment. This work was supported by a grant from the U.S. Department of Energy (DE-FG02-03ER15393). This is contribution 589 from the ASU Center for the Study of Early Events in Photosynthesis.

References and Notes

(1) McDermott, G.; Prince, S. M.; Freer, A. A.; Hawthornthwaite-Lawless, A. M.; Papiz, M. Z.; Cogdell, R. J.; Isaacs, N. W. *Nature* **1995**, *374*, 517−521.

(2) Koepke, J.; Hu, X.; Muenke, C.; Schulten, K.; Michel, H. *Structure* **1996**, *4*, 581−597.

(3) Burrell, A. K.; Officer, D. L.; Plieger, P. G.; Reid, D. C. W. *Chem. Rev.* **2001**, *101*, 2751−2796.

(4) Biemans, H. A. M.; Rowan, A. E.; Verhoeven, A.; Vanoppen, P.; Latterini, L.; Foekema, J.; Schenning, A. P. H. J.; Meijer, E. W.; de Schryver, F. C.; Nolte, R. J. M. *J. Am. Chem. Soc.* **1998**, *120*, 11054−11060.

(5) Cho, H. S.; Rhee, H.; Song, J. K.; Min, C.-K.; Takase, M.; Aratani, N.; Cho, S.; Osuka, A.; Joo, T.; Kim, D. *J. Am. Chem. Soc.* **2003**, *125*, 5849−5860.

(6) Takase, M.; Ismael, R.; Murakami, R.; Ikeda, M.; Kim, D.; Shinmori, H.; Furuta, H.; Osuka, A. *Tetrahedron Lett.* **2002**, *43*, 5157−5159.

(7) Kodis, G.; Liddell, P. A.; de la Garza, L.; Clausen, P. C.; Lindsey, J. S.; Moore, A. L.; Moore, T. A.; Gust, D. *J. Phys. Chem. A* **2002**, *106*, 2036−2048.

(8) Kuciauskas, D.; Liddell, P. A.; Lin, S.; Johnson, T. E.; Weghorn, S. J.; Lindsey, J. S.; Moore, A. L.; Moore, T. A.; Gust, D. *J. Am. Chem. Soc.* **1999**, *121*, 8604−8614.

(9) Gust, D. *J. Am. Chem. Soc.* **1977**, *99*, 6980−6982.

(10) Gust, D.; Fagan, M. W. *J. Org. Chem.* **1980**, *45*, 2511−2512.
(11) Patton, A.; Dirks, J. W.; Gust, D. *J. Org. Chem.* **1979**, *44*, 4749−4752.
(12) Maggini, M.; Scorrano, G.; Prato, M. *J. Am. Chem. Soc.* **1993**, *115*, 9798−9799.
(13) Hsiao, J.-S.; Krueger, B. P.; Wagner, R. W.; Johnson, T. E.; Delaney, J. K.; Mauzerall, D. C.; Fleming, G. R.; Lindsey, J. S.; Bocian, D. F.; Donohoe, R. J. *J. Am. Chem. Soc.* **1996**, *118*, 11181−11193.
(14) Lammi, R. K.; Ambroise, A.; Balasubramanian, T.; Wagner, R. W.; Bocian, D. F.; Holten, D.; Lindsey, J. S. *J. Am. Chem. Soc.* **2000**, *122*, 7579−7591.
(15) Liang, K.; Farahat, M. S.; Perlstein, J.; Law; K.-Y.; Whitten, D. G. *J. Am. Chem. Soc.* **1997**, *119*, 830−831.
(16) McRae, E. G.; Kasha, M. *Physical Processes in Radiation Biology*; Academic Press: New York, 1964; p 17.
(17) Luo, C.; Guldi, D. M.; Imahori, H.; Tamaki, K.; Sakata, Y. *J. Am. Chem. Soc.* **2000**, *122*, 6535−6551.
(18) Greaney, M. A.; Gorun, S. M. *J. Phys. Chem.* **1991**, *95*, 7241−7144.
(19) Kato, T. *Laser Chem.* **1994**, *14*, 155−160.
(20) Kuciauskas, D.; Liddell, P. A.; Moore, T. A.; Moore, A. L.; Gust, D. Solvent effects and electron-transfer dynamics in a porphyrin-fullerene dyad and a carotenoporphyrin-fullerene triad. In *Recent Advances in the Chemistry and Physics of Fullerenes and Related Materials*; Kadish, K. M., Ruoff, R. S., Eds.; The Electrochemical Society: Pennington, NJ, 1998; pp 242−261.
(21) Bell, T. D. M.; Jolliffe, K. A.; Ghiggino, K. P.; Oliver, A. M.; Shephard, M. J.; Langford, S. J.; Paddon-Row: M. N. *J. Am. Chem. Soc.* **2000**, *122*, 10661−10666.
(22) Williams, R. M.; Zwier, J. M.; Verhoeven, J. W. *J. Am. Chem. Soc.* **1995**, *117*, 4093−4099.
(23) Krasnovsky, A. A., Jr.; Bashtanov, M. E.; Drozdova, N. N.; Liddell, P. A.; Moore, A. L.; Moore, T. A.; Gust, D. *J. Photochem. Photobiol. A* **1997**, *102*, 157−161.
(24) Förster, T. *Ann. Phys.* **1948**, *2*, 55−75.
(25) Förster, T. *Discuss. Faraday Soc.* **1959**, *27*, 7−17.
(26) Wagner, R. W.; Johnson, T. E.; Lindsey, J. S. *J. Am. Chem. Soc.* **1996**, *118*, 11166−11180.
(27) Strachan, J. P.; Gentemann, S.; Seth, J.; Kalsbeck, W. A.; Lindsey, J. S.; Holten, D.; Bocian, D. F. *J. Am. Chem. Soc.* **1997**, *119*, 11191−11201.
(28) Du, H.; Fuh, R.-C. A.; Li, J.; Corkan, A.; Lindsey, J. S. *Photochem. Photobiol.* **1998**, *68*, 141−142.
(29) Yang, S. I.; Seth, J.; Strachan, J. P.; Gentemann, S.; Kim, D.; Holten, D.; Lindsey, J. S.; Bocian, D. F. *J. Porphyrins Phthalocyanines* **1999**, *3*, 117−147.
(30) Lindsey, J. S.; Brown, P. A.; Siesel, D. A. *Tetrahedron* **1989**, *45*, 4845−4866.
(31) Liddell, P. A.; Kuciauskas, D.; Sumida, J. P.; Nash, B.; Nguyen, D.; Moore, A. L.; Moore, T. A.; Gust, D. *J. Am. Chem. Soc.* **1997**, *119*, 1400−1405.
(32) Kuciauskas, D.; Liddell, P. A.; Lin, S.; Stone, S.; Moore, A. L.; Moore, T. A.; Gust, D. *J. Phys. Chem. B* **2000**, *104*, 4307−4321.
(33) Carbonera, D.; Di Valentin, M.; Corvaja, C.; Agostini, G.; Giacometti, G.; Liddell, P. A.; Kuciauskas, D.; Moore, A. L.; Moore, T. A.; Gust, D. *J. Am. Chem. Soc.* **1998**, *120*, 4398−4405.
(34) Kuciauskas, D.; Liddell, P. A.; Moore, A. L.; Moore, T. A.; Gust, D. *J. Am. Chem. Soc.* **1998**, *120*, 10880−10886.
(35) Imahori, H.; El-Khouly, M. E.; Fujitsuka, M.; Ito, O.; Sakata, Y.; Fukuzumi, S. *J. Phys. Chem. A* **2001**, *105*, 325−332.
(36) Kuciauskas, D.; Lin, S.; Seely, G. R.; Moore, A. L.; Moore, T. A.; Gust, D.; Drovetskaya, T.; Reed, C. A.; Boyd, P. D. W. *J. Phys. Chem.* **1996**, *100*, 15926−15932.
(37) Gust, D.; Moore, T. A.; Makings, L. R.; Liddell, P. A.; Nemeth, G. A.; Moore, A. L. *J. Am. Chem. Soc.* **1986**, *108*, 8028−8031.
(38) Osuka, A.; Yamada, H.; Shinoda, T.; Nozaki, K.; Ohno, O. *Chem. Phys. Lett.* **1995**, *238*, 37−41.
(39) Imahori, H.; Tamaki, K.; Araki, Y.; Sekiguchi, Y.; Ito, O.; Sakata, Y.; Fukuzumi, S. *J. Am. Chem. Soc.* **2002**, *124*, 5165−5174.
(40) Hush, N. S. *J. Chem. Phys.* **1958**, *28*, 962−972.
(41) Hush, N. S. *Trans. Faraday Soc.* **1961**, *57*, 557−580.
(42) Marcus, R. A. *J. Chem. Phys.* **1956**, *24*, 966−978.
(43) Marcus, R. A. *Can. J. Chem.* **1959**, *37*, 155−163.
(44) Imahori, H.; Hagiwara, K.; Akiyama, T.; Aoki, M.; Taniguchi, S.; Okada, T.; Shirakawa, M.; Sakata, Y. *Chem. Phys. Lett.* **1996**, *263*, 545−550.
(45) Guldi, D. M. *Chem. Soc. Rev.* **2002**, *31*, 22−36.
(46) Larsson, S.; Klimkans, A.; Rodriguez-Monge, L.; Duskesas, G. *J. Mol. Struct.* **1998**, *425*, 155−159.
(47) Imahori, H.; Hagiwara, K.; Aoki, M.; Akiyama, T.; Taniguchi, S.; Okada, T.; Shirakawa, M.; Sakata, Y. *J. Am. Chem. Soc.* **1996**, *118*, 11771−11782.
(48) Eaton, S. S.; Eaton, G. R. *J. Am. Chem. Soc.* **1975**, *97*, 3660−3666.
(49) Lindsey, J. S.; Prathapan, S.; Johnson, T. E.; Wagner, R. W. *Tetrahedron* **1994**, *50*, 8941−8968.
(50) Gust, D.; Moore, T. A.; Luttrull, D. K.; Seely, G. R.; Bittersmann, E.; Bensasson, R. V.; Rougée, M.; Land, E. J.; de Schryver, F. C.; Van der Auweraer, M. *Photochem. Photobiol.* **1990**, *51*, 419−426.
(51) Davis, F. S.; Nemeth, G. A.; Anjo, D. M.; Makings, L. R.; Gust, D.; Moore, T. A. *Rev. Sci. Instrum.* **1987**, *58*, 1629−1631.
(52) Freiberg, A.; Timpmann, K.; Lin, S.; Woodbury, N. W. *J. Phys. Chem. B* **1998**, *102*, 10974−10982.
(53) Golub, G. H.; Reinsch, C. *Numer. Math.* **1970**, *14*, 403−420.
(54) Henry, E. R.; Hofrichter, J. *Methods Enzymol.* **1992**, *210*, 129−192.